UCRL-JRNL- 206033

LAWRENCE
LIVERMORE
NATIONAL
LABORATORY

Spatially Resolved Spectra from a new X-ray Imaging Crystal Spectrometer for Measurements of Ion and Electron Temperature Profiles

M. Bitter, K. W. Hill, B. Stratton, A. L. Roquemore, and D. Mastrovito, S. G. Lee, and J. G. Bak, M. K. Moon, U. W. Nam, G. Smith, J. E. Rice, P. Beiersdorfer, B. S. Fraenkel

July 21, 2004

For submission to Review of Scientific Instruments

DISCLAIMER

This document was prepared as an account of work sponsored by an agency of the United States Government. Neither the United States Government nor the University of California nor any of their employees, makes any warranty, express or implied, or assumes any legal liability or responsibility for the accuracy, completeness, or usefulness of any information, apparatus, product, or process disclosed, or represents that its use would not infringe privately owned rights. Reference herein to any specific commercial product, process, or service by trade name, trademark, manufacturer, or otherwise, does not necessarily constitute or imply its endorsement, recommendation, or favoring by the United States Government or the University of California. The views and opinions of authors expressed herein do not necessarily state or reflect those of the United States Government or the University of California, and shall not be used for advertising or product endorsement purposes.

This is a preprint of a paper intended for publication in a journal or proceedings. Since changes may be made before publication, this preprint is made available with the understanding that it will not be cited or reproduced without the permission of the author.

Spatially Resolved Spectra from a new X-ray Imaging Crystal Spectrometer for Measurements of Ion and Electron Temperature Profiles

M. Bitter, K. W. Hill, B. Stratton, A. L. Roquemore, and D. Mastrovito
Plasma Physics laboratory, Princeton University, Princeton, New Jersey 08543

S. G. Lee, and J. G. Bak
Korea Basic Science Institute, Yusung, Taejeon 305-333, Korea

M. K. Moon
Korea Atomic Energy Research Institute, Yusung, Taejeon

U. W. Nam
Korea Astronomy Observatory, Yusung, Taejeon 305-348, Korea

G. Smith
Brookhaven National Laboratory, Upton, New York 11973

J. E. Rice
Plasma Science and Fusion Center, Massachusetts Institute of Technology, Massachusetts 02139

P. Beiersdorfer
Lawrence Livermore National Laboratory, Livermore, California 94550

B. S. Fraenkel
Hebrew University, Jerusalem, Israel

Abstract

A new type of high-resolution X-ray imaging crystal spectrometer is being developed to measure ion and electron temperature profiles in tokamak plasmas. The instrument is particularly valuable for diagnosing plasmas with purely Ohmic heating and rf heating, since it does not require the injection of a neutral beam - although it can also be used for the diagnosis of neutral-beam heated plasmas. The spectrometer consists of a spherically bent quartz crystal and a two-dimensional position-sensitive detector. It records spectra of helium-like argon (or krypton) from multiple sightlines through the plasma and projects a de-magnified image of a large plasma cross-section onto the detector. The spatial resolution in the plasma is solely determined by the height of the crystal, its radius of curvature, and the Bragg angle. This new X-ray imaging crystal spectrometer may also be of interest for the diagnosis of ion temperature profiles in future large tokamaks, such as KSTAR and ITER, where the application of the presently used charge-exchange spectroscopy will be difficult, if the neutral beams do not penetrate to the plasma center. The paper presents the results from proof-of-principle experiments performed with a prototype instrument at Alcator C-Mod.

I. Introduction

A new X-ray imaging crystal spectrometer, which can record temporally and spatially resolved spectra of helium-like ions from multiple sightlines through the plasma, has been proposed for the measurement of ion and electron temperature profiles in tokamak plasmas.[1,2] The spectrometer consists of a spherically bent crystal and a two-dimensional position-sensitive detector. The elements of interest are medium-Z elements from argon to krypton, which are present in tokamak plasmas as indigenous impurities or which are injected as trace elements for diagnostic purposes. Other potential diagnostic applications of this new instrument include measurements of rotation velocity profiles and measurements of the profiles of the ionization equilibrium, which are of interest for impurity transport studies.

One of the main advantages of the X-ray imaging crystal spectrometer resides in the fact that it can provide data for all experimental conditions, which include plasmas with purely Ohmic heating as well as plasmas with rf and neutral-beam heating, and that - contrary to diagnostics based on neutral charge exchange recombination spectroscopy – injection of a neutral beam is not required. The spectrometer may therefore also be attractive for the diagnosis of the core ion temperature in future large tokamaks, such as KSTAR[3] and ITER[4], where the application of charge exchange recombination spectroscopy may be compromised by a reduced penetration of neutral beams to the plasma center. One may also expect that this new instrument will replace the presently used arrays of single-chord X-ray crystal spectrometers,[5,6] reducing costs, saving precious diagnostic space, and - at the same time - providing more reliable profiles with better spatial resolution, since a cross-calibration of spectra from different sightlines is not needed due to the fact that all the spectra are produced by Bragg reflection from the same spherically bent crystal.

A prototype instrument, which consisted of a spherically bent crystal and a conventional one-dimensional multi-wire counter and which recorded spectra from only a central sightline through the plasma, was operating at NSTX during the period from 2000 to 2002. These early experiments already demonstrated the applicability of a spherically bent crystal, and they provided valuable data for performance estimates of a fully equipped X-ray imaging crystal spectrometer. In particular, it was found that ion and electron temperature measurements could be performed in rf heated plasmas at NSTX with a time resolution of 10 ms, using only small, non-perturbing argon gas puffs.[7] The experimental results obtained have also set new benchmarks for theoretical calculations of the dielectronic satellite spectra of helium-like ions and, in particular, ArXVII,[8] since it was found that the widely used theoretical predictions of Vainshtein et al.[9] for the intensity ratios for the $n = 2$ and $n \geq 3$ dielectronic satellites with respect to the ArXVII resonance line were not in agreement with the experimental data for a unique value of the electron temperature, i.e. different values for the electron temperature were obtained depending on whether it was derived from the $n = 2$ and $n \geq 3$ dielectronic satellites. The resulting uncertainties for the electron temperature measurements were more than 20%, for electron temperatures below 1 keV, causing an unacceptable uncertainty for the evaluation of the power balance of NSTX plasmas. This problem was resolved by a recalculation of the auto-ionization probabilities and branching ratios for the $n = 2$ and $n \geq 2$ satellites with new atomic physics code.[10] The synthetic spectra constructed from this new code are now in full agreement with the observed spectra, yielding a unique value for the electron temperature from all the spectral features. Moreover, the electron temperature values obtained are also in good agreement with the results from Thomson scattering.[8] The improved theoretical calculations of the new

atomic physics code[9] may also be of interest for the interpretation of helium-like spectra from astrophysical observations.

Since 2002, the development of the spectrometer is being funded by a grant from the US Department of Energy.[11] This grant has made it possible to equip the spectrometer with two, two-dimensional, position-sensitive, 10 cm x 30 cm, multi-wire proportional counters, which are used alternately. Both detectors have delay-line readouts, which are a cost-efficient and elegant electronic solution. One of the detectors and a PC based data acquisition system were developed by the Korea Basic Science Institute (KBSI) in collaboration with the Korea Atomic Energy Research Institute (KAERI) and the Korea Astronomy Observatory (KAO) for future use with the crystal spectrometers at KSTAR.[12,13] The other detector was built at the Brookhaven National Laboratory (BNL).[14] This detector has a better spatial resolution; but it became only recently available, and it is presently not quite compatible with the data acquisition system, so that only a restricted area of 6 cm x 18 cm of this detector can be presently used. Multi-wire proportional counters were considered to be the appropriate choice for proof-of-principle experiments, since they can be readily built to any desired size based on proven technology. They have also a very high signal-to-noise ratio, good spatial resolution, and a detection efficiency close to 100% for X-ray energies of 3keV, if krypton is used as a detector gas. However, different types of large area detectors will be needed in the future to increase the throughput and dynamic range of the spectrometer, since the count rate of multi-wire proportional counters for single photon counting is limited to about 400 kHz. It is thought that the development of new detector concepts will be guided by the results obtained with the present multi-wire proportional counters. Because of the early termination of the NSTX experimental campaign in 2003, the spectrometer was temporarily transferred to Alcator C-Mod, where it was in operation during the period from June 2003 to November 2003. The paper presents the results obtained from these proof-of principle experiments at Alcator C-Mod.

II. Design Concept of the new X-ray Imaging Crystal Spectrometer

The type of spectrometer, which is most widely used on tokamak experiments, is the Johann crystal spectrometer,[15] consisting of a cylindrically bent crystal and a one-dimensional position-sensitive detector, which are placed on the Rowland circle as shown in Fig. 1 of reference 16. The Johann spectrometer is a focusing device for the so-called meridional rays in the main dispersion plane. As illustrated in Fig. 1 of reference 16, the meridional rays, which are emitted from point sources on the Rowland circle, are reflected and focused to corresponding points on the Roland circle if the Bragg condition is satisfied, so that an entire spectral range can be observed simultaneously. Since each spectral line is produced by Bragg reflection from the entire crystal, measurements of line intensity ratios are not affected by non-uniformities of the crystal and they can therefore be performed with high accuracy and high throughput. Although X-rays of different wavelengths are emitted from different volume elements of the plasma, there are certain preferred experimental arrangements on tokamaks - see Fig. 1 in reference 16 – for which the different volume elements are equivalent, due to the fact that the electron temperature and therefore the X-ray emissivity are constant in the direction of the toroidal magnetic field. The distance between crystal and plasma can be arbitrarily chosen due to the fact that a Johann spectrometer does not require a slit. This instrumental feature facilitates the fielding of a Johann spectrometer at a tokamak experiment. Although the Johann configuration has optimal focusing properties for the meridional rays, it does not provide any focusing for the so-called sagittal rays, which are oblique to the main dispersion plane. The typical Johann spectrometer can therefore

only be used to record spectra from a single sightline through the plasma. Arrays of single-chord crystal spectrometers have been used in the past to measure profiles of plasma parameters.[5,6] However, due to the large size of high-resolution X-ray crystal spectrometers such arrays included only a small number instruments, so that the spatial resolution obtained was rather coarse.

This longstanding problem can be solved by replacing the cylindrically bent crystal in the Johann geometry with a spherically bent crystal and by using the astigmatism of a spherical mirror as described in reference 1. Because of the astigmatism of a spherical mirror, the meridional and sagittal rays originated from a point source on the Rowland circle and reflected from the mirror are focused at different points, F_m and F_s, respectively; F_m is always on the Rowland circle, while the distance of F_s from the crystal can vary between $-\infty$ and $+\infty$, depending on the Bragg angle Θ.[1] For $45° < \Theta < 90°$, the reflected sagittal rays converge to a point F_s in front of the mirror. For $0° < \Theta < 45°$, the reflected sagittal rays are divergent and seem to originate from a virtual focus F_s behind the mirror. For $\Theta = 45°$, F_s is at infinity, so that – if we consider the imaging properties for the reversed rays – a parallel bundle of sagittal rays originating from the plasma is focused onto a point on the Rowland circle. Parallel bundles of sagittal rays, which are inclined to the main dispersion plane are focused to points above or below the main dispersion plane, so that it is possible to focus the radiation from different regions of the plasma to different points on a detector. These conditions are still approximately fulfilled for Bragg angles near 45°, e. g. Θ = 54° used in our experiment, since the sagittal rays, which are emitted from the plasma and then Bragg reflected from the crystal, appear to emerge from a distant point F_s. The spatial resolution in the plasma is thus solely determined by the height of the crystal, its radius of curvature, and the Bragg angle. Note that the imaging properties are rotationally symmetric about the normal of the crystal, so that the incident and reflected rays form a cone about the normal of the crystal. The traces of the spectral lines on the detector are therefore curved and determined by the intersections of the corresponding Bragg cones with the detector plane. We point out that the X-ray imaging crystal spectrometer, which is discussed in this paper, will only function for extended plasma sources, such as tokamaks.

III. Experimental arrangement at Alcator C-Mod

The experimental arrangement of the spectrometer at Alcator C-Mod was similar to the arrangement at NSTX shown in Fig. 1 of reference 7, except that the distance between crystal and plasma was equal to the distance between crystal and detector, so that a 1:1 image of the plasma was projected onto the detector. Moreover, the field of view was restricted by the 8 in. wide port on Alcator C-Mod to a plasma cross-section extending from –9 cm below to +9 cm above the horizontal mid-plane. The spectrometer was equipped with a new spherically bent 110 quartz crystal with a 2d-spacing of 4.913 Å and the before-mentioned Korean two-dimensional position-sensitive detector with a delay-line readout and a PC-based data acquisition system.[12,13] The crystal was a circular disk with a diameter of 100 mm and a radius of curvature of 3888 mm. The mean Bragg angle for the observed spectral range, which extended from the ArXVII resonance line $1s^2\ S_0 - 1s2p\ ^1P_1$ (w) at 3.9494 Å to the ArXVII forbidden line $1s^2\ S_0 - 1s2s\ ^3S_1$ (z) at 3.9944 Å, was θ_0 = 54°; and the images, F_m and F_s, formed by the meridional and sagittal rays from an imaginary point source on the Rowland circle would, therefore, appear at distances of 3125 mm and 10172 mm from the crystal – see equation (1) in reference 1. Under these conditions, the spatial resolution in the plasma was about 0.7 times the height of the crystal. A rather new experience was the high radiation intensity at Alcator C-Mod, which tended to

saturate our detector. In order to avoid saturation of the detector by the Bragg reflected bremsstrahlung and ArXVII line radiation, the crystal had to be masked, so that the exposed crystal area was only 8 mm (wide) x 3 mm (high), resulting in a high spatial resolution of 2 mm in the plasma. We point out that Alcator C-Mod is a high-density machine and that the radiation intensity is proportional to the square of the density. On NSTX as on most other tokamaks, the radiation intensity is smaller by about two orders of magnitude compared to Alcator C-Mod, so that on NSTX an effective crystal area of 60 mm (wide) x 40 mm (high) has been used without saturating the detector – see Fig. 2 in reference 7.

The data acquisition system consisted of a Time to Digital Converter (TDC N110),[17] which was specifically designed for two-dimensional multi-wire counters with delay-line readout, and an interface between the TDC and a PC. The TDC determines - with a time resolution of 156 ps - the time-delays of the four signals from the ends of the two 290 ns delay-lines of the detector with respect to a common start signal. The start signal is derived from a special plane of coarsely spaced wires in the detector. The x- and y-coordinates on the detector are calculated for each photon and presented as two 2-byte words at the out put of the TDC. The interface, consisting of a TMS320VC33 digital signal processor, a 16 Mbytes static memory, and supporting Windows OS image software, determines the arrival time T of each photon with respect to a trigger pulse at the beginning of each plasma discharge with a time resolution of 33 ns and transfers the combined (X, Y, T) information for each photon as a single word to the PC. It is, therefore, possible to bin the data in time groups and spatial groups of interest after a plasma discharge, at the time of the data analysis.

IV. Experimental results from Alcator C-Mod

Figure 1 shows a typical time-integrated raw data spectrum as displayed on the PC terminal of the data acquisition system at the end of an Alcator C-Mod discharge. The wavelength is displayed on the horizontal x-axis, while the height of the X-ray emitting plasma sections from the horizontal mid-planed is given on the vertical y-axis. The spectral range extends from the ArXVII resonance line w at 3.9494 Å to the ArXVII forbidden line **z** at 3.9944Å. The field of view was restricted in the y-direction for the longer wavelengths due to vignetting by the 8 in. wide access port, so that the height of the observed plasma cross-section decreased from $\pm$ 9 cm for the line **w** to and $\pm$ 5 cm for the line **z**. The white horizontal lines are the shadows from the supporting metal ribs for the beryllium entrance window of the detector. These lines provide a convenient scale for the analysis of the spectral data, since the ribs are 10 mm apart.[12] As expected, the spectral lines are curved due to the afore-mentioned rotational symmetry of the Bragg reflection about the normal of the crystal.

Figure 2 presents an accumulated spectrum from five nearly identical Alcator C-Mod discharges. The spectral data have been collapsed on the x-axis. The spectral features are very well defined and have been identified with use of Gabriel's notation.[18] The 'apparent' ion temperature derived from the width of the line **w** of the collapsed spectrum is 2.1 keV. This value is higher than the 'true' ion temperature, since no corrections were made for the curvature of the spectral lines.

Figure 3 shows an overlay of the total photon count rates as a function of time from five similar Alcator C-Mod plasmas. Argon was injected at 0.3 s. Note that the detector is in saturation during the period from 0.5 to 1.7 s, even though the exposed crystal area had been reduced to a small section of 8 mm x 3 mm. The usable time interval is therefore restricted to the period from 0.3 to

0.5 s, where the detector is not yet saturated. The increase of the observed count rate during the interval from 1.3 s to 1.6 s is due to rf heating of these Alcator plasmas during this time interval. However, since the detector was in saturation, the actual count rate during this period may have been considerably higher than the observed count rate. The fact that use of a tiny crystal was sufficient to saturate the detector/electronics in our experiments at Alcator C-Mod argues favorably for the suitability of these spectrometers for use on ITER; thus neutron collimators with small cross-sectional area can be used to minimize neutron streaming to the crystal.

Figure 4 shows spatially resolved spectra of the resonance line **w** and associated $n \geq 3$ satellites during the time interval from 350 to 450 ms. The figure was produced by binning the spectral data in five, 4 cm wide y-segments for the fixed range of channel numbers from 120 to 200 in the x-direction - see Fig. 2. The spectra have been analyzed by a least-squares fit comparison with synthetic spectra constructed from the theoretical predictions by Vainshtein.[9] The theoretical wavelength of 3.9494 Å for the resonance line **w** was assigned to the channel number, which corresponds to the center position of the peak. Doppler shifts of the observed spectral lines due to a toroidal rotation of the plasma can be excluded, since the sightlines for the entire spectrum were to within 1° parallel to a major radius of the plasma, i. e. perpendicular to the toroidal direction. The relative shifts of the spectra in adjacent y-bins must, therefore, be ascribed to the rotational symmetry of the imaging properties about the normal of the crystal. The values for the ion and electron temperatures, which were obtained from the Doppler width of the resonance line **w** and the satellite-to-resonance line ratios, are listed in Fig. 4. It is evident from Fig. 4 that the line widths and satellite-to-resonance line ratios as well as the line intensities in the five spectra shown are similar, and the ion and electron temperature results obtained from the fit of these data are therefore not very different. Similar results were obtained from a more detailed analysis of the data – see Figure 5, which shows the ion and electron temperature values obtained from the spectra in 1 cm wide y-segments for the range from –10 cm to +10 cm at two different time intervals. These experimental results indicate that the temperature profiles were rather flat over the field of view from –10 cm to +10 cm. These results were also confirmed by independent measurements of the electron cyclotron emission with a Grating Poly-Chromator, which yielded the electron temperature profile in the outer half of the plasma column in the horizontal mid-plane – see Fig. 6. According to these measurements the electron temperature profile was flat over the central region from 68 to 74 cm. In order to obtain an estimate for the Alcator C-Mod electron temperature profile in a direction perpendicular to the horizontal mid-plane, the profile shown in Fig. 6 must be stretched by an elongation factor of 1.7. The temperature profiles obtained from the X-ray Imaging Crystal Spectrometer are, therefore, in good agreement with those from the Grating Poly-Chromator. We point pout that all the spectral data were obtained from Alcator C-Mod discharges with plasma currents of 800 kA. Low-current (I_p < 800 kA) discharges have steeper ion and electron temperature profiles. However, no experiments with low-current discharges were performed at Alcator C-Mod during the time of our visit.

Another important result from the experiments at Alcator C-Mod is that the observed curvature of the spectral lines was found to be in excellent agreement with theoretical expectations. Due to the rotational symmetry of imaging properties the incident and Bragg reflected X rays form a cone about the normal of the crystal, so that the observed curvature of the spectral lines should be given by the intersection of the corresponding cones with the detector plane. The curves of intersection should be hyperbolas for Bragg angles $\theta < 45°$, parabolas for $\theta = 45°$, and ellipses for $\theta > 45°$. In our case, the curves of intersection should be ellipses, since the Bragg angles are near 54°. The

parameters of these ellipses should be different for each spectral line, since each wavelength corresponds to a different Bragg angle. Figure 7 shows the observed center position (X-coordinate) for the spectral lines **w** and **z** as a function of the Y-coordinate on the detector and, for comparison, an overlay of the ellipses derived from the above-mentioned geometrical considerations. In order to reduce the statistical error for determination of the center position of the spectral lines, the spectral data had been binned in 1 cm wide segments in Y-direction. The major and minor half axes of the theoretically expected ellipses are **a** = 5012 mm and **b** = 3414 mm for the line **w** at 3.9494 Å and **a** = 4729 mm and b = 3262 mm for the line **z** at 3.9944 Å. The distance between the lines **w** and **z,** which encompass the entire spectrum of interest, was 49 mm at the center of the detector. Although the ellipses for the lines **w** and **z** have different parameters, it turns out that the differences between these ellipses over the relatively small area of the detector are smaller than the detector resolution, if they are overlaid with each other. It is, therefore, justified to describe the curvature of all the spectral lines by *only one* ellipse, using the ellipse for the mean Bragg angle of 53.95°. One can then determine the relative shift of the spectra in adjacent Y-bins from a cross-correlation calculation by integration over the entire spectral range from **w** to **z**. The cross-correlation method has the advantage that the statistical error is significantly reduced, so that it is possible to determine the relative line shifts for very small y-segments. Figure 7 presents results obtained from the cross-correlation method. The experimental data had been binned in 2.5 mm wide segments in the Y-direction. The theoretical curve, which is shown for comparison, represents the ellipse for a central wavelength between **w** and **z** at the Bragg angle $\theta = 53.95°$. Since the observed and theoretically expected line shifts are in excellent agreement, we may conclude that the imaging properties of this spherical crystal spectrometer have been experimentally verified.

V. Future Plans

The experiments at Alcator C-Mod have made it very clear that it is absolutely necessary to develop large, high count rate (multi-MHz) detectors in order to increase the dynamic range of the spectrometer and to make it a useful diagnostic for a wide range of tokamak experiments. This project is pursued in several ways: As the most affordable and practical solution for the near future it is planned to develop large, segmented two-dimensional position-sensitive multi-wire proportional counters in collaboration with the Korean Laboratories. A long-term solution may be expected from the development of large area, Gas Electron Multiplication (GEM) detectors[19] with fast delay line readouts. Multi-wire proportional counters and the GEM detectors are most suitable for X-ray energies below 10 keV. For the measurement of krypton lines at 13 keV in future large tokamaks such as KSTAR and ITER, it may be possible to use large-aperture TV detectors similar to those, which are presently being developed at the European Synchrotron Facility in collaboration with Hamamatsu.[20]

Our plans for the immediate future are to optimize the presently available equipment for the measurement of ion and electron temperature profiles at NSTX with high spectral and spatial resolution. The BNL detector is being modified, so that it will be fully compatible with the interface of our data acquisition system. This modification will allow us to make use of the full 10 cm x 30 cm area of the BNL detector and to image an 80 cm high cross-section of the plasma on the detector with a demagnification factor of 2.5. Since the BNL detector has a good spatial resolution of less than 0.2 mm, it will be possible to measure ion temperatures below 1 keV in the edge region of the plasma with sufficient accuracy. Of particular interest are the temperature profiles in low-current NSTX discharges with appreciable gradients over the spectrometer's field of view.

Acknowledgements
We gratefully acknowledge the support of the US Department of Energy through Contract DE-AC02-76-CHO-3073 and Grant 1083 for the Development of Advanced Plasma Diagnostics. Work by the University of California Lawrence Livermore National Laboratory was performed under the auspices of the U.S. DOE under contract W-7405-Eng-48.

References

(1) M. Bitter, K. W. Hill, A. L. Roquemore, P. Beiersdorfer, S. M. Kahn, S. R. Elliot, and B. S. Fraenkel, Rev. Sci. Instrum. **70**, 292 (1999)

(2) US Patent 6,259,763 B1 2001

(3) S. G. Lee et al., Poster C06 at this conference

(4) R. Barnsley et al., Poster C23 at this conference

(5) M. Bitter, K. W. Hill, S. von Goeler, et al., Rev. Sci. Instrum. **57**, 2145 (1986)

(6) J. E. Rice and E. S. Marmar, Rev. Sci. Instrum. **61**, 2753 (1990)

(7) M. Bitter, K. W. Hill, L. Roquemore,P. Beiersdorfer, A. Thorn, and Ming Feng Gu, Rev. Sci. Instrum. **74**, 1977 (2003)

(8) M. Bitter, M. F. Gu, L. A. Vainshtein, P. Beiersdorfer, G. Bertschinger, O. Marchuk. R. Bell, B. LeBlanc, K. W. Hill, D. Johnson, and L. Roquemore, Phys. Rev. Lett. **91**, 265001-1

(9) L. A. Vainshtein and U. I. Safronova, At. Data Nucl. Data Tables **21**, 49 (1978); **25**, 311 (1980)

(10) M. F. Gu, Astrophys. J. **582**, 1241 (2003)

(11) US Department of Energy Program Announcement LAB 01-25: *Development of Diagnostic Systems for Magnetic Fusion Energy Sciences, Contract No. 1083*

(12) S. G. Lee, J. G. Bak, M. Bitter, M. K. Moon, U. W. Nam, K. C. Jin, K. N. Kong, and K. I. Seon, Rev. Sci. Instrum. **74**, 1997 (2003)

(13) U. W. Nam, K. N. Kong, Y. S. Park, Y. J. Kim, S. G. Lee, J. G. Bak, M. Bitter, K. W. Hill, and M. K. Moon, Bull. Am. Phys. Soc., October 2003, Volume 48, No. 7, Poster BP1 4, p. 32

(14) G. C. Smith, B. Yu, J. Fischer, V. Radeka, and J.A. Harder, Nucl. Instrum. & Meth. A323, 78-85 (1992)

(15) H. H. Johann, Z. Phys. **69**, 185 (1931)

(16) M. Bitter, S. von Goeler, R. Horton, M. Goldman, K. W. Hill, N. R. Sauthoff, and W. Stodiek, Phys. Rev. Lett. **42**, 304 (1979)

(17) C. Hervé, European Synchrotron Radiation Facility, http://www.esrf.fr/computing/cs/csel/released/s110/n110.html

(18) A. H. Gabriel, Mon. Not, R, Astron. Soc., **160**, 99 (1972)

(19) http://ts-dep-dem.web.cern.ch/ts-dep-dem/products/gem/

(20) Y. Amemiya, K. Ito, . Yagi,Y. Asano, K. Wakabayashi, T. Ueki, and T. Endo, Rev. Sci. Instrum. **66**, 2290 (1995)

Figure Captions

Figure 1: Time integrated spectrum of helium-like argon, ArXVII, from an Alcator C-Mod discharge as displayed on the PC terminal of the data acquisition system after the discharge. The wavelength is given on the horizontal axis (x-axis), and the location of the X-ray emitting plasma region is given on the vertical axis (y-axis).

Figure 2: Accumulated spectrum from five nearly identical Alcator C-Mod discharges. The spectral data have been collapsed on the x-axis. The spectral features have been identified with use of Gabriel's notation.[18]

Figure 3: Overlay of the total count rates as a function of time from the same five Alcator C-Mod discharges.

Figure 4: Spatially resolved spectra of the ArXVII resonance line and associated $n \geq 3$ dielectronic satellites from the same five discharges during the time interval from 350 to 450 ms. The spectral data have been binned in five 4 cm wide y-segments for the fixed range of channel numbers from 120 to 200 in the x-direction – see Fig. 2. the theoretical wavelength of 3.9494 Å for the resonance line was assigned to the channel corresponding to the center position of the main peak. Also shown are the results from least-squares fit comparisons of the data with synthetic spectra constructed from theoretical predictions.[9]

Figure 5: Ion and electron temperature results obtained from the spectral data in 1 cm wide y-segments for the time intervals from 400 to 500 ms and from 500 to 600 ms.

Figure 6: Outer half of the electron temperature profile in the horizontal mid-plane at 600 ms from the Alcator C-Mod discharge 111402, which was one of the five above-mentioned discharges. The data have been obtained from measurements of the electron cyclotron emission with a Grating Poly-Chromator.

Figure 7: X-coordinate of the lines **w** and **z** as a function of the y-coordinate on the detector and overlay of the theoretically expected ellipses, for comparison. The data have been binned in 1 cm wide y-segments. The major and minor half axes of the ellipses are **a** = 5012 mm (and 4729 mm) and **b** = 3414 mm (and 3262 mm) for the lines **w (**and **z**), respectively.

Figure 8: Displacement of spectral data along the x-axis as a function of the y-coordinate on the detector as determined from the cross-correlation of the spectral data in adjacent 2.5 mm wide y-segments. Also shown is an overlay of the theoretically expected ellipse for a mean Bragg angle of $\theta = 53.95°$.

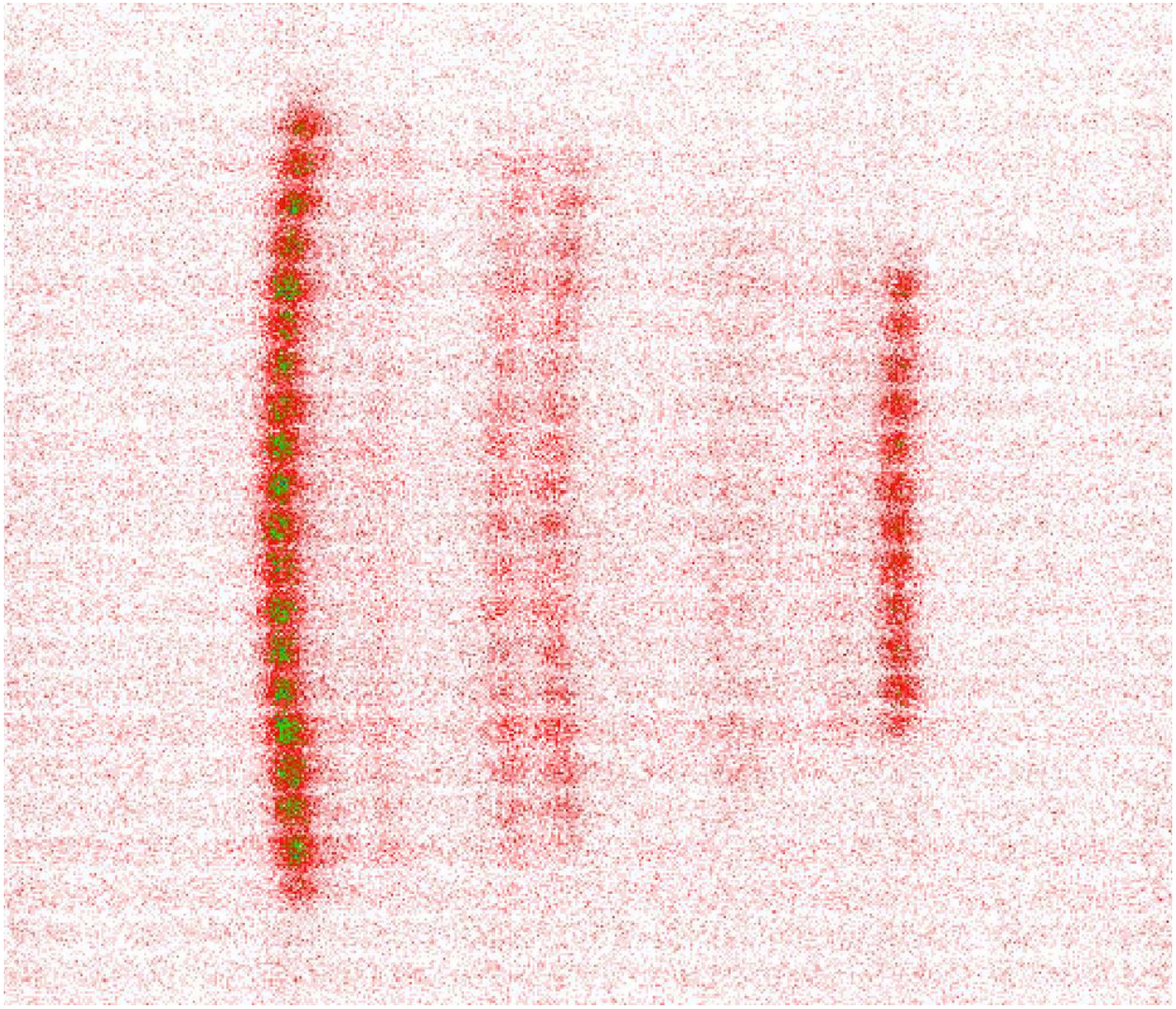

Figure 1

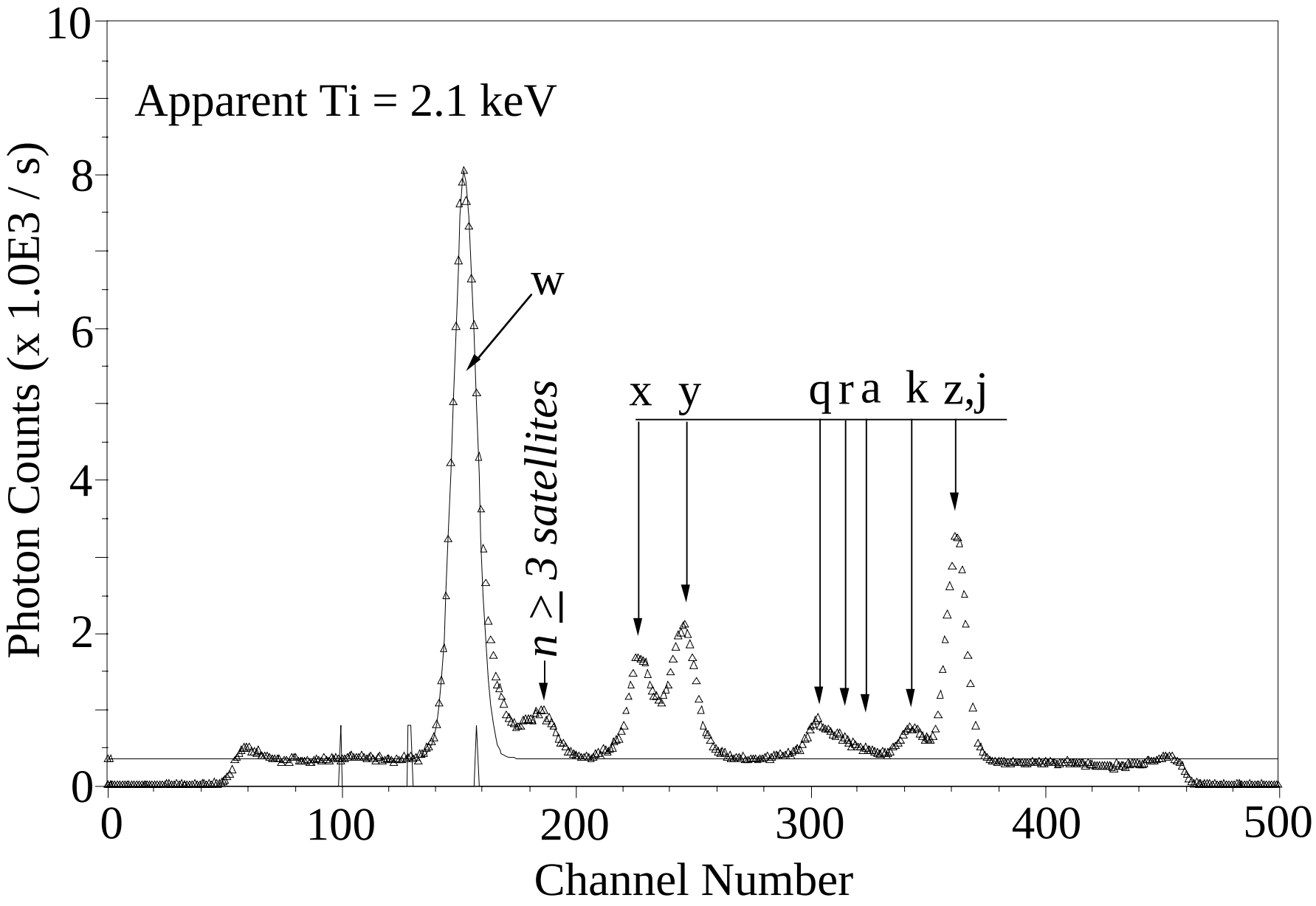
Apparent Ti = 2.1 keV
w
x y
q r a k z,j
n ≥ 3 satellites
Photon Counts (x 1.0E3 / s)
Channel Number
0
2
4
6
8
10
0
100
200
300
400
500

Figure 2

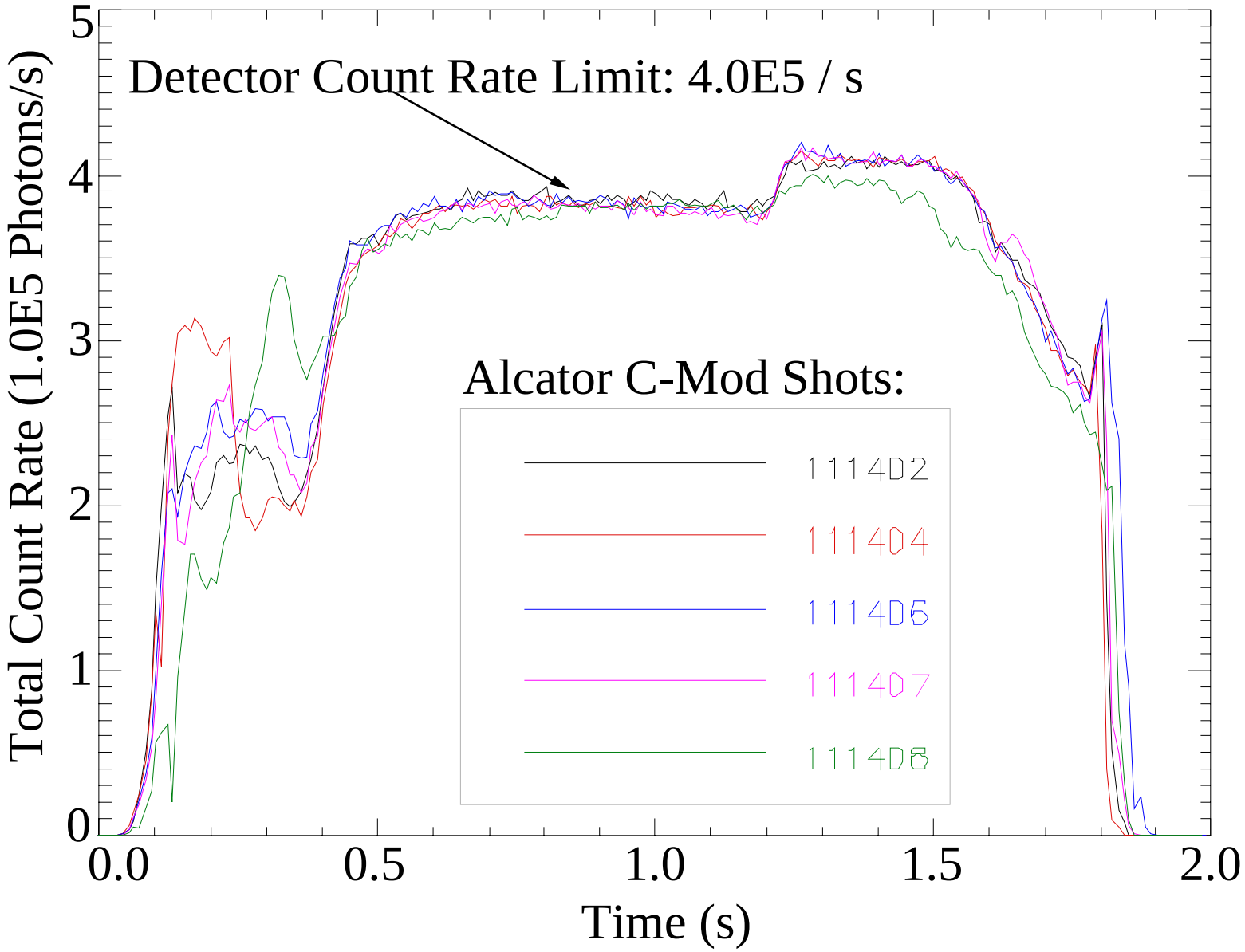
Detector Count Rate Limit: 4.0E5 / s
Alcator C-Mod Shots:
111402
111404
111406
111407
111408
Total Count Rate (1.0E5 Photons/s)
Time (s)
0
1
2
3
4
5
0.0
0.5
1.0
1.5
2.0

Figure 3

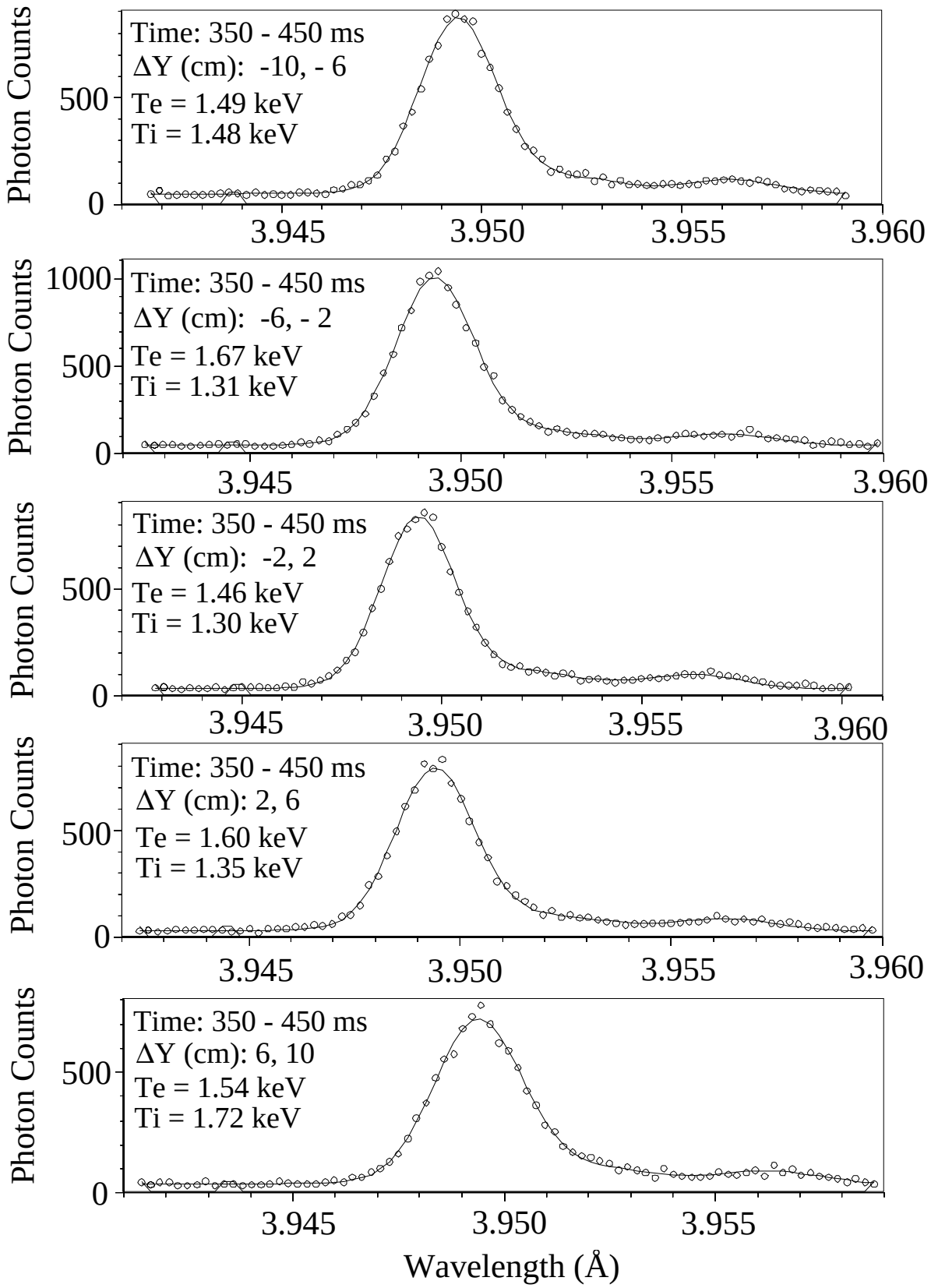
Time: 350 - 450 ms
ΔY (cm): -10, - 6
Te = 1.49 keV
Ti = 1.48 keV
Time: 350 - 450 ms
ΔY (cm): -6, - 2
Te = 1.67 keV
Ti = 1.31 keV
Time: 350 - 450 ms
ΔY (cm): -2, 2
Te = 1.46 keV
Ti = 1.30 keV
Time: 350 - 450 ms
ΔY (cm): 2, 6
Te = 1.60 keV
Ti = 1.35 keV
Time: 350 - 450 ms
ΔY (cm): 6, 10
Te = 1.54 keV
Ti = 1.72 keV
Photon Counts
0
500
1000
3.945
3.950
3.955
3.960
Wavelength (Å)

Figure 4

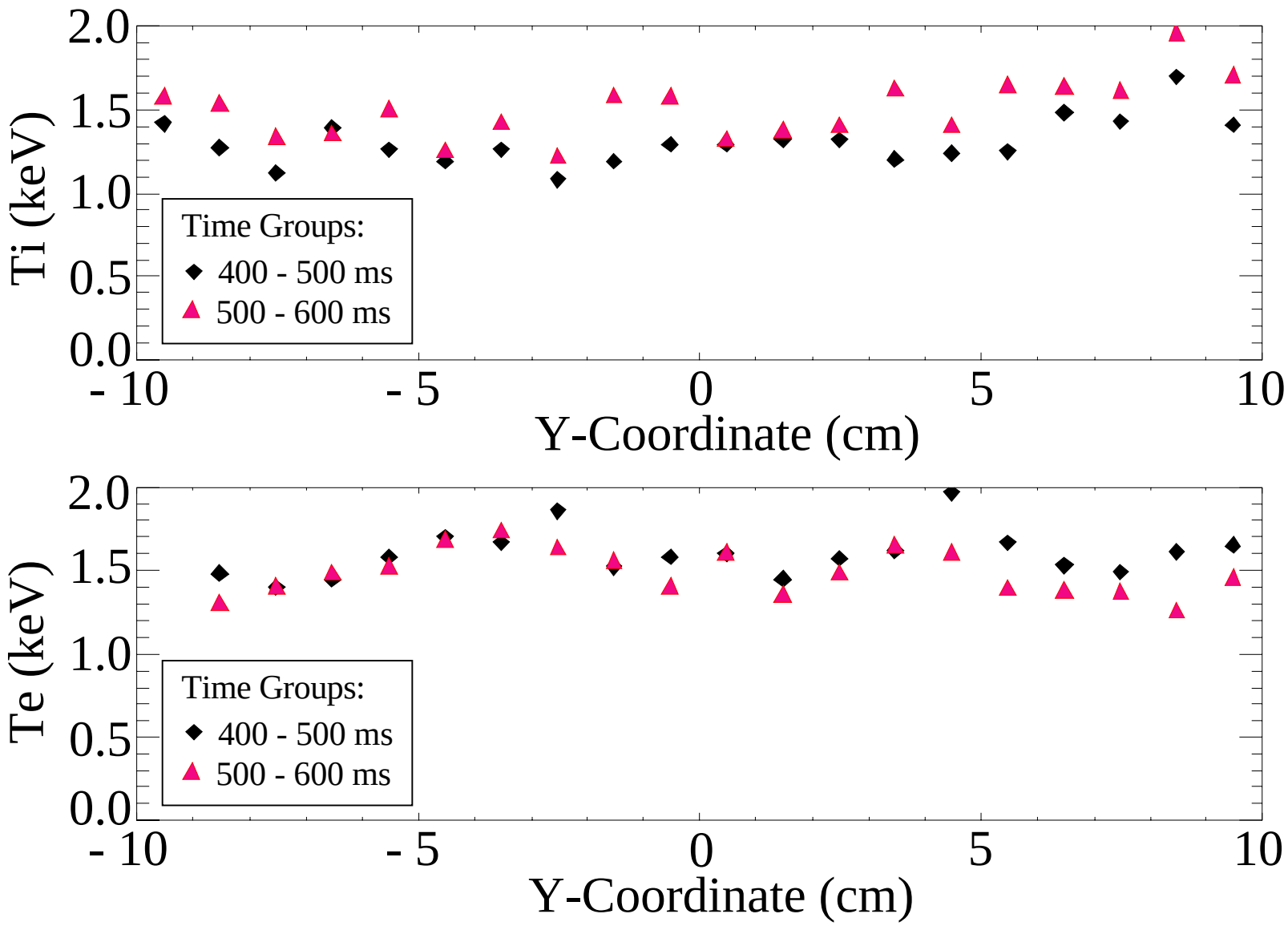
2.0
1.5
1.0
0.5
0.0
Ti (keV)
Time Groups:
400 - 500 ms
500 - 600 ms
- 10
- 5
0
5
10
Y-Coordinate (cm)
2.0
1.5
1.0
0.5
0.0
Te (keV)
Time Groups:
400 - 500 ms
500 - 600 ms
- 10
- 5
0
5
10
Y-Coordinate (cm)

Figure 5

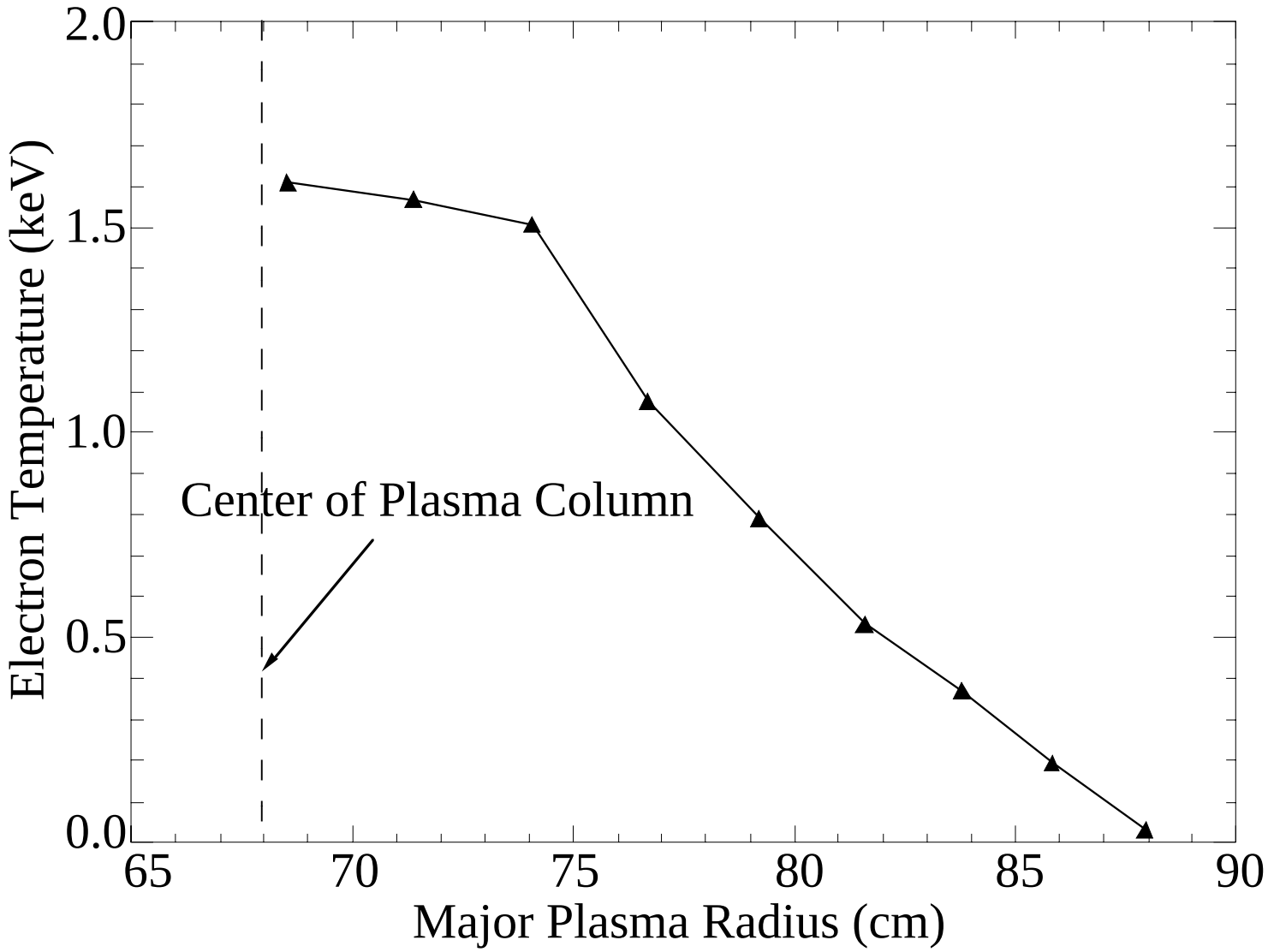
2.0
1.5
1.0
0.5
0.0
Electron Temperature (keV)
Center of Plasma Column
65
70
75
80
85
90
Major Plasma Radius (cm)

Figure 6

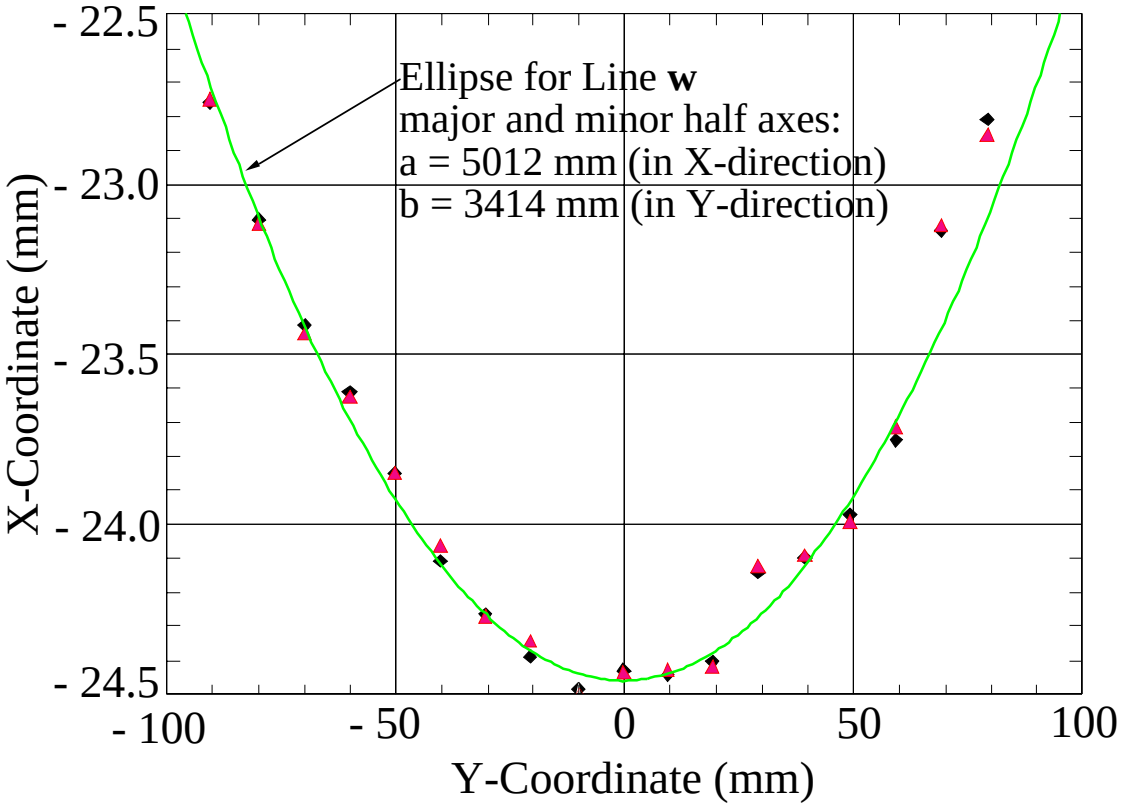
Ellipse for Line **w**
major and minor half axes:
a = 5012 mm (in X-direction)
b = 3414 mm (in Y-direction)
X-Coordinate (mm)
Y-Coordinate (mm)
- 22.5
- 23.0
- 23.5
- 24.0
- 24.5
- 100
- 50
0
50
100

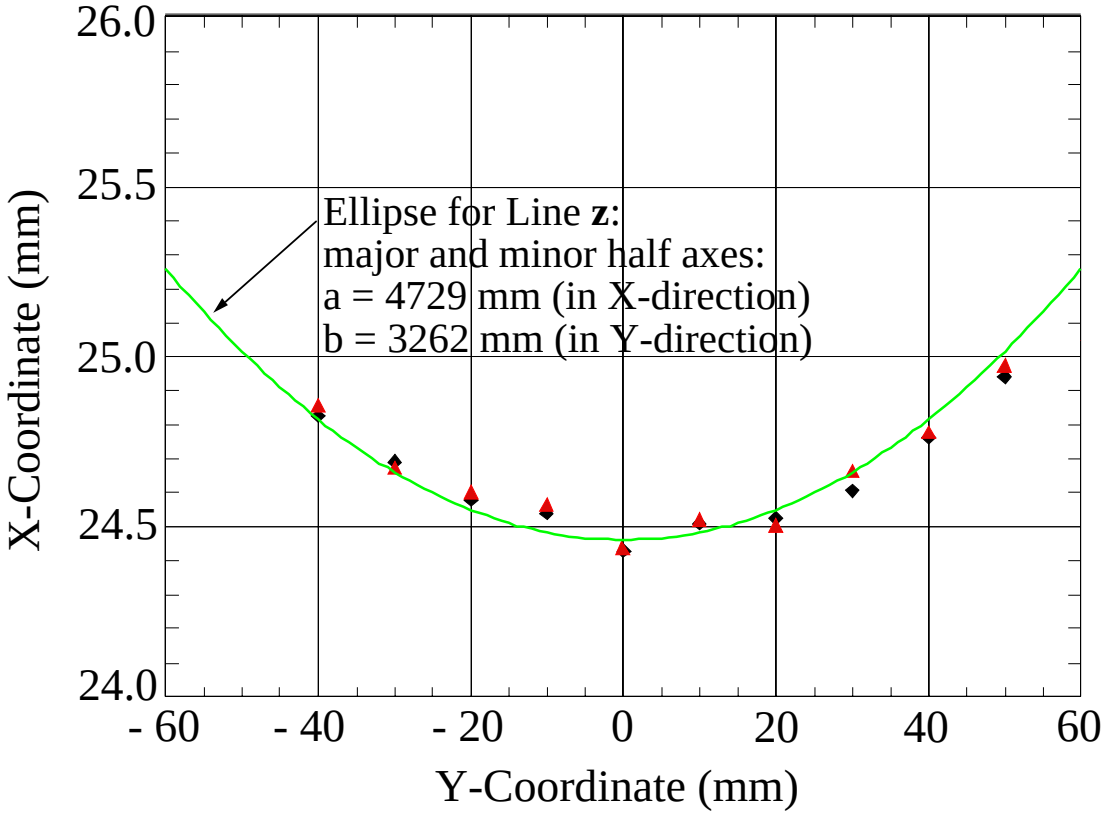
Ellipse for Line **z**:
major and minor half axes:
a = 4729 mm (in X-direction)
b = 3262 mm (in Y-direction)
X-Coordinate (mm)
Y-Coordinate (mm)
26.0
25.5
25.0
24.5
24.0
- 60
- 40
- 20
0
20
40
60

Figure 7

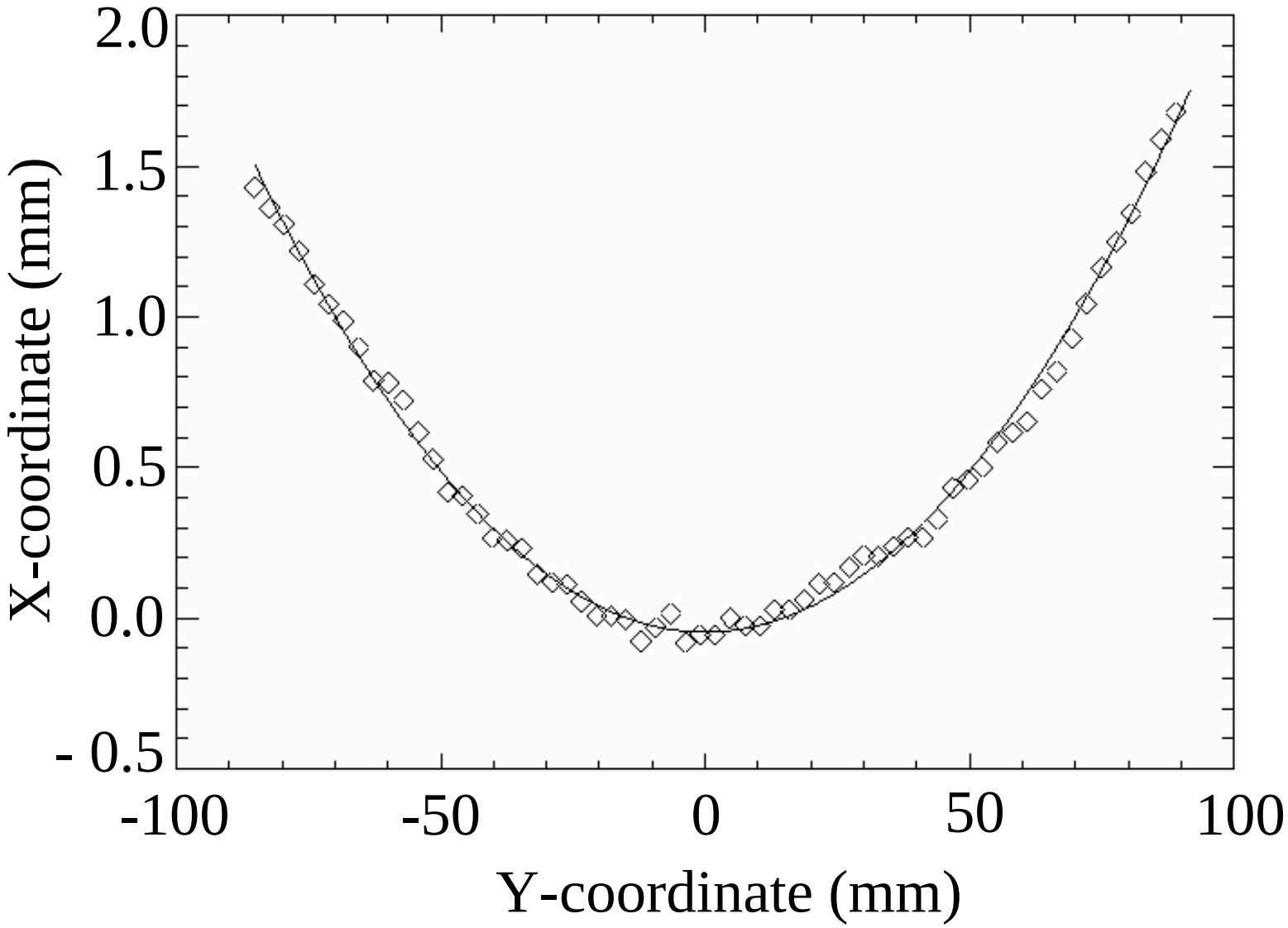

Figure 8

University of California
Lawrence Livermore National Laboratory
Technical Information Department
Livermore, CA 94551